P7.8

NEW HAIL DIAGNOSTIC PARAMETERS DERVIED BY INTEGRATING MULTIPLE RADARS AND MULTIPLE SENSORS

Gregory J. Stumpf[1,2,], Travis M. Smith[1,3], James Hocker[1,3]*

[1]Cooperative Institute for Mesoscale Meteorology Studies, University Of Oklahoma, Norman, Oklahoma.
[2]NOAA/National Weather Service/Meteorological Development Laboratory, Silver Spring, Maryland.
[3]NOAA/National Severe Storms Laboratory, Norman, Oklahoma.

1. INTRODUCTION

Numerous National Weather Service (NWS) Weather Forecast Office (WFO) local studies (Amburn and Wolf 1997, Billet et al 1997, Blaes et al 1998, Hart and Frantz 1998, Lenning et al 1998, Roeseler and Wood 1997, Troutman and Rose 1997, Turner and Gonsowski 1997) and national studies (Edwards and Thompson 1998, Witt et al 1998, Witt 2002) looked at the relationship between various conventional radar- and environmentally-derived parameters for severe hail diagnosis in storms. A variety of different parameters have been used:

- Vertically Integrated Liquid (VIL)
- VIL Density
- Hail Diagnosis Algorithm (HDA; Witt et al 1998) parameters:
  - Severe Hail Index (SHI)
  - Probability of Severe Hail (POSH)
  - Maximum Expected Hail Size (MEHS)
- Height of the 50 dBZ level above the ground (e.g., 50 dBZ Echo Tops)
- Reflectivity at 0°C and -20°C
- Height of the 50 dBZ Reflectivity above 0°C and -20°C
- Maximum Vertical Reflectivity (a.k.a. Composite Reflectivity)
- Height of the Maximum Reflectivity
- Height of the wet bulb zero ($H_{Tw = 0°C}$).

Most of these parameters are derived from single radar Weather Surveillance Radar – 1988 Doppler (WSR-88D) Open Radar Products Generator (ORPG) products, either from gridded fields or from cell-based attributes from the Storm Cell Identification and Tracking algorithm (SCIT; Johnson et al 1998) and the HDA.

The ORPG is limited in that it cannot integrate data from multiple-radars or multiple-sensors - in this case, Near-Storm Environment (NSE) data from mesoscale numerical models (e.g., RUC20). Therefore, any of these parameters which require environmental thermodynamic information must be determined by mentally integrating radar data with the NSE data – sometimes difficult to do for all storms for each volume scan. Also, when storms are under-sampled by a single radar (e.g., cones-of-silence, far ranges), attributes that are derived by vertically-integrating reflectivity (e.g., VIL, SHI) typically do not represent the true values in the storms, and in many cases are underestimated.

The National Severe Storms Laboratory (NSSL) Warning Decision Support System – Integrated Information (WDSSII; Hondl 2002, Lakshmanan 2003) provided a development environment to integrate data from multiple-radars and multiple-sensors to rapidly prototype some new applications to diagnose hail in storms, including all of the parameters in the above list. The following manuscript will detail the status and progress of this work done collaboratively between the NWS Meteorological Development Laboratory (MDL) and NSSL.

2. HAIL DIAGNOSIS PARAMETERS

2.1 Vertically Integrated Liquid (VIL)

VIL is a radar-derived estimate of liquid water (exclusive of ice) that is computed using the following equation (Greene and Clark 1972):

$$\text{VIL (kg m}^{-2}) = \sum 3.44 \times 10^{-6}[(Z_i + Z_{i+1})/2]^{4/7} \Delta h \qquad (1)$$

To exclude contributions of ice from VIL, if $(Z_i + Z_{i+1})/2 >$ 56 dBZ, it is set to 56 dBZ. Note that VIL is designed to remove contamination by ice, yet it is still widely used as predictor for hail! In fact, a popular practice is for forecasters to use a "VIL-of-the-Day" threshold for hail warning. Typically, the first few hail reports are correlated with the VIL of the storm, and the threshold is adjusted accordingly. It is usually observed that VILs-of-the-Day are typically lower (higher) in colder (warmer) air masses. Amburn and Wolf (1997) point out the limitations of using this practice, especially in light of varying strength and depths of storms observed during the same time within a radar domain.

VIL products are available in three formats to NWS forecasters: 1) A 4 km × 4 km Cartesian grid in which the vertical integration is performed for the data within the volume above that grid square. For each elevation scan, the maximum reflectivity intersecting the volume is

*Corresponding Address: c/o NOAA/National Severe Storms Laboratory, 1313 Halley Circle, Norman, OK, 73069. Tel: 405-366-0477, Fax: 405-366-047, Email: greg.stumpf@noaa.gov

used to derive the VIL, 2) A "High-Resolution VIL (HRVIL, or Digital VIL, or DVIL)", a 1° × 1 km polar grid (same resolution of the native reflectivity data), in which the vertical integration is also performed for the data within the volume above the grid area (after all elevation scan data has been remapped to a 0° elevation earth-tangent plane). In this case, the actual value of reflectivity for each elevation scan for the sample volume with the same range and azimuth is used to derive VIL, 3) Cell-based VIL from the SCIT algorithm. For each elevation scan, the maximum reflectivity of the 2D storm component used to create the 3D storm detection is used to derive VIL.

There are strengths and limitations with all three methods for computing VIL. Most obvious is the fact that tilted reflectivity cores will be sampled differently using all three methods. Clearly, the cell-based VIL is preferred if a user wants to maximize the VIL values along a tilted (and perhaps "twisted") reflectivity core, as the maximum reflectivities are always used in the integration (Fig. 1). Plus, cell-based attributes can be trended over time in graphical format. This, of course, assumes that the SCIT algorithm is correctly identifying the entire storm in the vertical and has stable tracks. Recent studies by the ROC and NSSL have shown that this is not always the case. The heuristic and centroid-based methods used in the SCIT algorithm can be unstable and can be subject to small fluctuations in reflectivity value and location, this leading to incorrect vertical and time associations and broken trends.

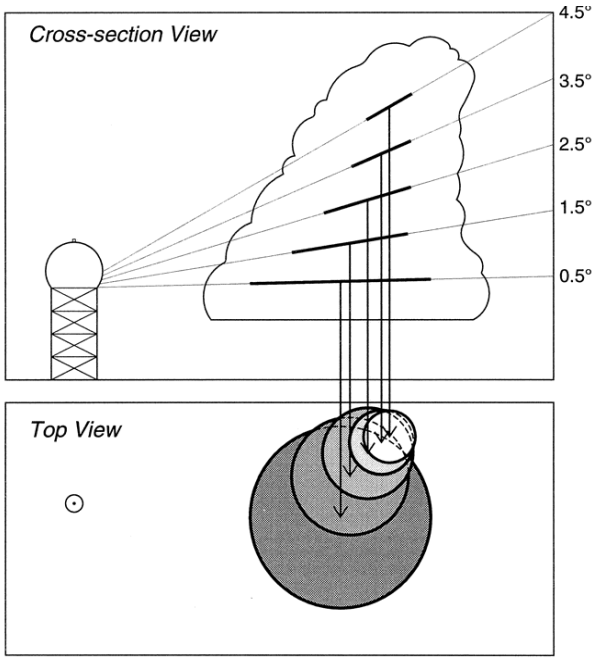

Fig. 1: Diagram illustrating the identification of 2D storm components (thick lines and circles) within a cell by the SCIT algorithm.

Comparing the two gridded products – the chances of a 4 km × 4 km grid volume intersecting with the maximum reflectivities in a tilted or twisted core are much greater than on the 1° × 1 km polar grid, and thus you'd expect higher VILs on the 4 km × 4 km grid. Gridded products offer geospatial information on VIL maxima – in other words, one knows where in the storm the maximum VIL is, rather than one VIL value per storm as is available with cell-based VIL. The disadvantage is that VIL trends cannot be easily extracted for trends graphs, but must be inferred using animation of VIL images over time.

As of this writing, the HRVIL product does not have a 56 dB*Z* upper limit when integrating reflectivities. Some recent evaluations have shown that on average, the HRVIL values are higher than the 4 km × 4 km VIL values in storms, even though the vertical column of integration is smaller. A future build of HRVIL will incorporate the 56 dB*Z* upper limit to match the 4 km × 4 km VIL computations, and thus we'd expect that average values of HRVIL will decrease. The reduction in average HRVIL should be most noticeable at close range where the vertical columns are most narrow.

2.2 VIL Density

The traditional VIL Density (VD) formula used by NWS meteorologists is simply the value of VIL divided by the "echo top" (ET) height (Amburn and Wolf 1997):

$$VD\ (g\ m^{-3}) = 1000 * VIL\ (kg\ m^{-2}) / ET\ (m) \qquad (2)$$

A VIL Density product is unavailable from the ORPG, so meteorologists will compute it manually using two methods. A gridded VIL Density can be computed by comparing the gridded VIL product to the gridded "Echo Tops" ORPG product. The present Echo Tops products is determined by the maximum height of the occurrence of 18 dB*Z* in the vertical profile of reflectivity from all elevation scans that intersect the vertical "box" centered over a 4 km × 4 km grid square. An Enhanced Echo Tops (EET) product is now available which computes the Echo Top values on a 1° × 1 km polar grid. Also, the values are integrated between elevation scans rather than given as the height of the data from the nearest elevation scan (this removes "rings" in the echo tops product). However, the EET product is too new to have been used in any recent VIL Density studies (at least, none have yet to be published).

A cell-based VIL Density can also be manually computed from the cell-based VIL and "Cell Top" products available from SCIT. It is important to remember that the cell-based VIL product is based on maximum reflectivities within a tilted and twisted reflectivity core, and can typically be higher than grid-based VILs. Also, the Cell Top product in SCIT is based upon the height of the top 2D storm component used to create the 3D cell detection. The 2D component must meet a reflectivity threshold of 30 dB*Z* or greater (instead of 18 dB*Z*), and the area of the component must exceed 10 km^2 (versus the size of a grid pixel, either 4 km × 4 km or 1° × 1 km). Also, the height of the component is equivalent to the height of elevation scan data at the range of the component centroid (there is no

interpolation to the next higher elevation scan, as in the EET product). Some of the studies have shown that cell-based VIL Densities are not as robust as the grid based densities.

A common limitation of a gridded VIL density as reported by several studies is that for strongly sheared storms or for storms which are moving relatively fast (e.g., > 15 m s^{-1}), the storms will appear tilted in the vertical due to the ascending elevation scan sampling (Amburn and Wolf 1997, Hart and Frantz 1998). This can result in the Echo Top being horizontally offset from the main reflectivity core by one or more grid locations. For some studies, the maximum Echo Top value within one grid location, in any direction of the maximum VIL, was used to determine the VIL Density.

VIL Density was designed to "normalize" the VIL values based on storm height and is determined to be a better alternative than VIL-of-the-Day hail threshold practices (Amburn and Wolf 1997). The hypothesis states that equivalent VIL values in shorter storms mean higher likelihood of severe hail. However, Troutman and Rose (1997) infer the reason that VIL Density appears to provide better hail guidance is because shorter high-VIL storms are typically associated with cold-season environments, with lower melting layers, which results in a higher-likelihood for hail anyway. Furthermore, warm-season low-topped storms may show high VIL densities, even though these storms are typically not severe hail producers (the microphysics are dominated by warm rain processes below the melting level).

2.3 Hail Diagnosis Algorithm (HDA) products

The WSR-88D Hail Detection Algorithm (HDA; Witt et al 1998), now referred to as the Hail Diagnosis Algorithm (Witt, personal communication) is a diagnostic extension to the SCIT algorithm (Johnson et al 1998). It is based on single-radar data, and is cell-based, meaning only one set of hail attributes are available per storm cell per volume scan. The algorithm logic is based on a similar integration of reflectivity values in the vertical. However, in contrast to VIL which is designed to reduce "hail contamination" by forcing all reflectivity values to be less than or equal to 56 dB*Z* during the integration, the HDA uses a parameter known as the Severe Hail Index (SHI) which includes higher reflectivity values in the integration. No reflectivities below 40 dB*Z* are used, all reflectivities above 50 dB*Z* are used, and reflectivities between 40 and 50 dB*Z* are linearly weighted from 0 to 1 (a proxy to the curve shown in Fig. 2). Furthermore, only reflectivities (meeting the above criteria) above the melting layer are considered. Reflectivities between the 0°C and -20°C levels are weighted from 0 to 1, and all reflectivities (meeting the above criteria) above the -20°C level are considered. In essence, the integration is searching for hail cores aloft, a precursor to hail at the ground.

SHI is used to derive a Probability of Severe Hail (POSH) and Maximum Expected Hail Size (MEHS) based on the equations in Witt et al (1998), using the maximum reflectivities in the 2D SCIT components. There is anecdotal evidence that the cell-based HDA has a tendency to over warn for hail, but studies by Lenning et al (1998) and Witt (2000) seem to contradict this. They each state that the HDA is probably the best application currently available for hail diagnosis, at least for the local data sets they tested.

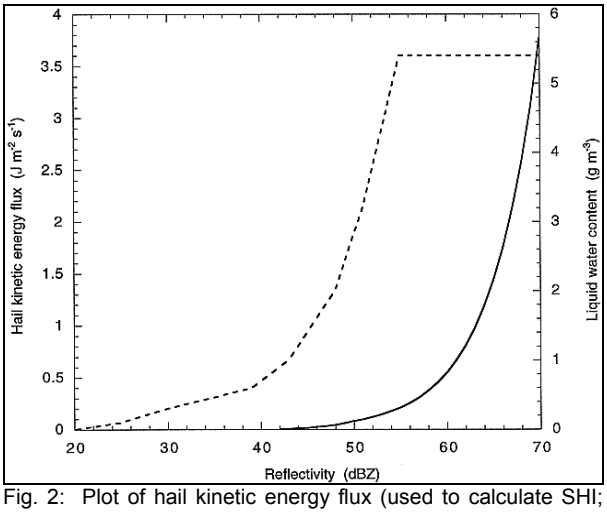

Fig. 2: Plot of hail kinetic energy flux (used to calculate SHI; solid curve), and liquid water content (used to calculate VIL; dashed curve), as a function of reflectivity.

More recent work with the HDA has included information about low-altitude relative humidity (to account for hail melting) storm-top divergence, mid-altitude rotation, and other kinematic and thermodynamic environmental parameters, which are then incorporated into a neural network prediction equation for an Enhance Hail Diagnosis Algorithm (EHDA; Marzban and Witt 2002).

2.4 Other popular parameters synthesized by manual base data interpretation

Several forecast offices have determined that their "best practices" are to not use any of the algorithm output (e.g., VIL, HDA) and instead manually diagnose the reflectivity data at various vertical levels in the storms. A combination of the D2D "All Tilts" browser or 4-panel displays along with data sampling are used to diagnose the maximum reflectivity for storms. While it is understandable to use manual methods to diagnose storms, especially in light of some of the algorithm limitations, these manual methods are typically very simple versions of some of the sophistication built into the algorithms, and have been shown to offer less predictive value than the algorithms (Lenning et al 1998). Furthermore, it is often a challenge for a meteorologist to keep up with every storm on every elevation and volume scan to conduct this analysis, and because of this, sometimes storms are improperly warned (either false, missed, or late). Some of these diagnoses are more properly completed by integrating radar data with environmental data (e.g., 0°C and -20°C

levels). Furthermore, any analysis using just single radar data will suffer from the limitations of under-sampling in certain parts of the radar domain.

One popular method is to determine the height of certain high reflectivity values (e.g., 50 dBZ) above the ground – in other words, a manually-determined 50 dBZ Echo Top. Also popular is to determine the reflectivity at various thermo-dynamic levels (e.g., 0°C and -20°C) or to compare the height of the 50 dBZ Echo Top to those thermodynamic heights. The HDA Severe Hail Index does exactly this and more. Not only are these values determined automatically, but high-reflectivity (> 40 - 50 dBZ) information is integrated for all elevations above the freezing level. Again, in contrast to VIL which is designed to remove hail contamination, the SHI is designed to include those reflectivities that contribute to the hail echo but in a more-sophisticated method. What may cause meteorologists to shy away from the HDA is that the SHI, and the intermediate output that is used to determine the SHI, is not available (as a sanity check). Also, the HDA output is only available in cell-based form, and grid-based versions of the product (like VIL) that provide geospatial hail information (and that don't suffer from the SCIT limitations) are not yet operationally available.

2.5 Height of the wet-bulb zero ($H_{Tw = 0°C}$)

All references and anecdotal evidence of use of this parameter in hail warning have not revealed how the radar data and radar attributes are integrated with this parameter to discriminate between storms producing or not producing severe hail. The references indicate that if the $H_{Tw = 0°C}$ is between a certain height range, the probability for hail in storms is increased, but no further information relating the parameter to radar data is presented. Therefore, this avenue is not pursued.

3. PROTOTYPES OF NEW MULTIPLE-SENSOR HAIL DIAGNOSIS PRODUCTS FOR AWIPS

First, we address the issue of multiple-radar integration. Multiple-radars offer better diagnosis of storms by over-sampling them, especially in single-radar cones-of-silence, at far ranges from one radar, and in areas where terrain is blocking the beams from one radar [which limited the studies of Amburn and Wolf (1997) and Edwards and Thompson (1998), among others]. Multiple-radar over-sampling also has the effect of reducing, on average, the height estimates of radar information such as echo top levels. An example of the benefits of multiple radar data integration is shown in Figure 3. Pictured is a comparison of one storm's cell-based VIL trend for a storm which passes through the cone-of-silence of a single radar. The single-radar trend shows a "trough" of VIL values, while from the multiple-radar trend we see that the storm VIL *peaked* during its passage through the cone-of-silence. The contribution of data from other radars provided a more-robust estimate of the VIL.

NSSL has developed a multi-radar mosaicking application that integrates data from multiple radars. The radar data is in its the original full resolution (8-bit) and full volume Level-II format as opposed to single radar Level III and IV 4-bit products which placed limitations on the studies by Amburn and Wolf (1997), Troutman and Rose (1997) and Hart and Frantz (1998), among others. The Level-II multiple-radar data are combined into a rapidly-updating 3D grid (the grids can be updated as fast as each new elevation scan update from one of the radars in the grid). Grid point locations sensed by more than one radar are assigned values based on various distance and time weighting schemes. Radar data that is several minutes old is also advected using a sophisticated scheme that clusters reflectivity features at different size scales and comparing these cluster images to images from previous times.

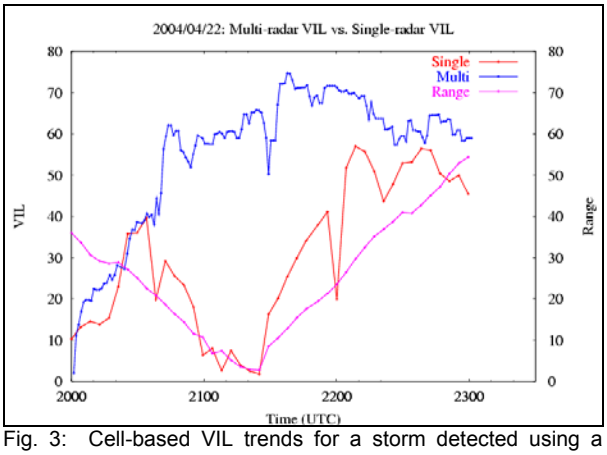

Fig. 3: Cell-based VIL trends for a storm detected using a single radar (red) and using multiple radars (blue). The range of the storm from the single radar is shown in magenta.

For the purposes of these prototypes, we have developed 3D gridded reflectivity data on a latitude-longitude-height grid with time and space dimensions approximately 1 km × 1 km × 1 km × 60 seconds. This radar grid also facilitates integration with other grids, such as mesoscale model grids. Thus, the multiple-radar 3D grids are integrated with RUC20 derived grids (e.g., 0°C and -20°C heights) which are bilinearly interpolated to a 1 km × 1 km grid and updated every 3600 seconds (1 hour).

Using the multiple-radar 3D grids, and in some cases the RUC20 derived grids, the following new products were developed. For these examples, the case of 222453 UTC 20 May 2001, integrating data from KTLX, KINX, and KSRX, is used. This case included two supercells in eastern Oklahoma which were associated with large hail and several tornadoes.

3.1 Vertically Integrated Liquid (VIL)

This VIL is computed in the same manner as the ORPG gridded VIL and HRVIL products except using the 1 km × 1 km × 1 km 3D multiple-radar grid. Since the 3D radar grid is updated every 60 seconds, this VIL product

is rapidly updated 4-5 times faster than either of the two ORPG products. VIL information is also more accurately depicted in areas where single radar data are under-sampling the storms. An example VIL grid is shown in Fig. 4a, along with the multiple-radar reflectivity data from the 3D grid at the 1000m AGL level (Fig 4b). Another version of the VIL product with no upper dBZ limits (to emulate the present build of the HRVIL) is shown in Fig. 4c. Note that only a few grid values are higher, mainly in the cores and peak values of the storms.

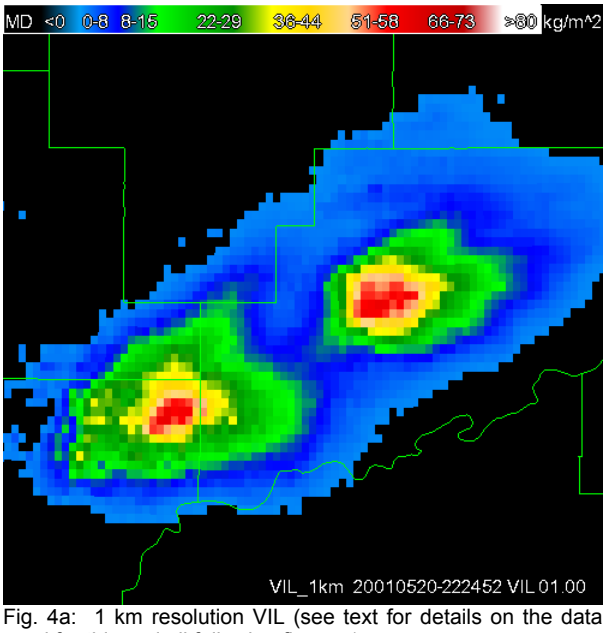

Fig. 4a: 1 km resolution VIL (see text for details on the data used for this and all following figures.)

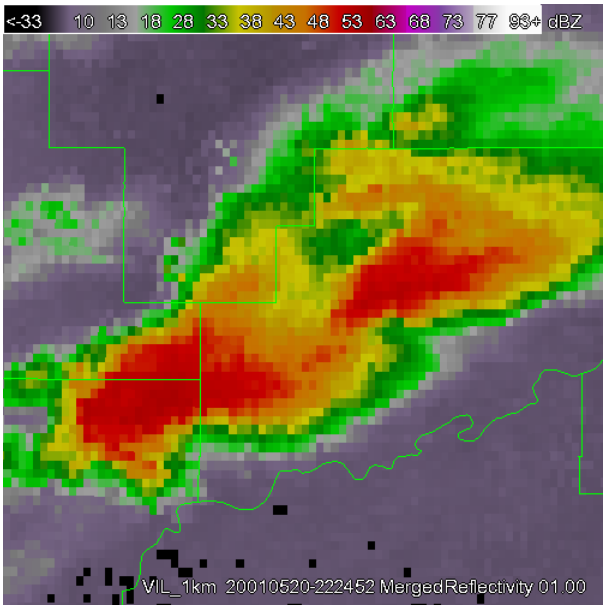

Fig. 4b: Multi-radar Reflectivity (1000m AGL)

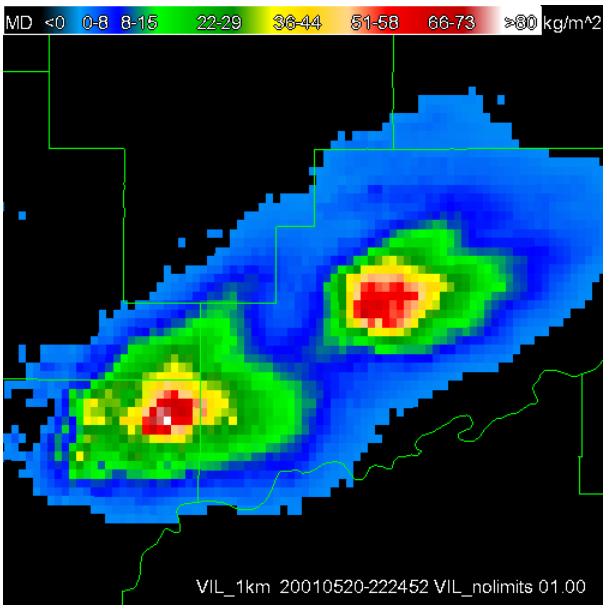

Fig. 4c: 1 km resolution VIL without the upper 56 dBZ limit

3.2 Echo Tops (18 dBZ, 30 dBZ, 50 dBZ)

These echo top products are computed by determining the maximum height (AGL) of the occurrence of several reflectivity levels in the vertical profile of reflectivity from all vertical grid points over each 1 km × 1 km grid square. The height is interpolated between the 1 km vertical levels. The 18 dBZ Echo Tops (EchoTop_18; Fig. 5a) are computed as a proxy to the ORPG Echo Tops and EET products, and is used for the VIL Density gridded product (see below). The 30 dBZ Echo Tops (EchoTop_30; Fig. 5b) are computed as a proxy to the SCIT "Cell Top" product (although no consideration is made for an area threshold of 10 km^2 as in SCIT). The 50 dBZ Echo Tops (EchoTop_50; Fig. 5b) are computed because they are popular products used with manual base data interpretation practices.

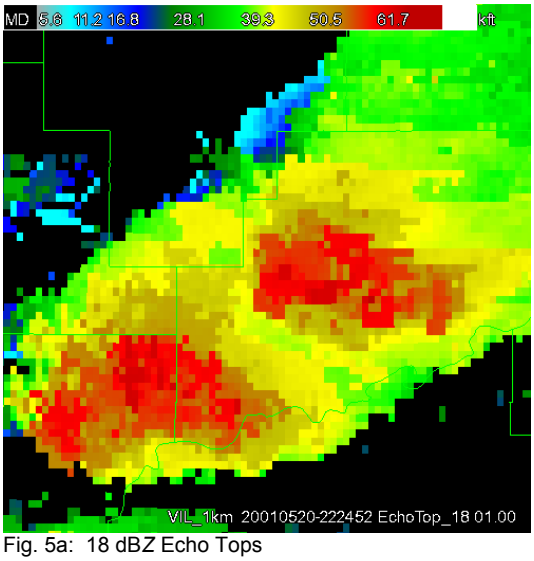

Fig. 5a: 18 dBZ Echo Tops

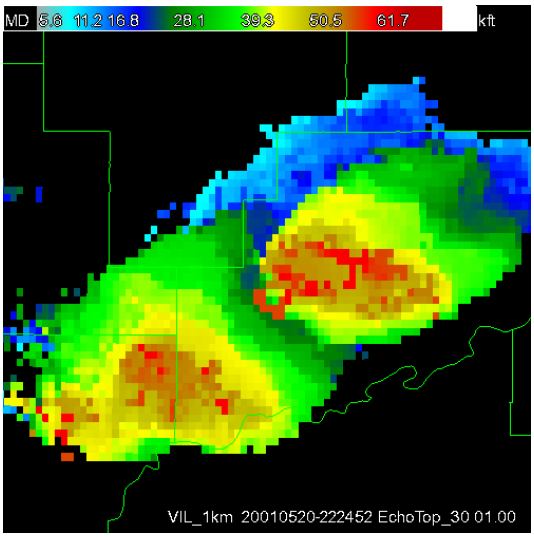

Fig. 5b: 30 dBZ Echo Tops

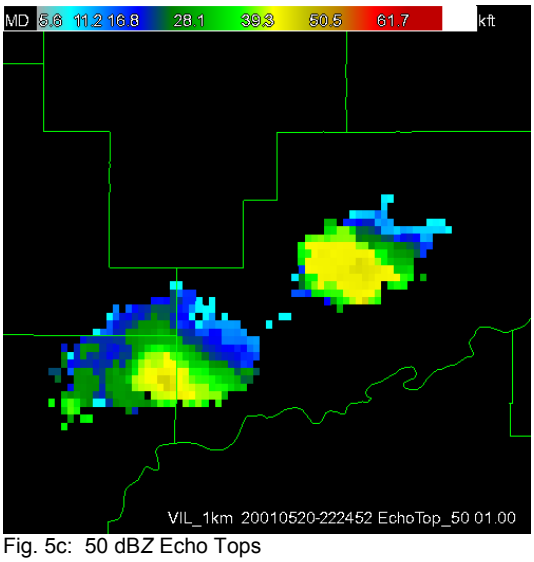

Fig. 5c: 50 dBZ Echo Tops

3.3 VIL Density

This multiple-radar VIL Density product is computed using Eq. (2), by dividing the gridded VIL value with the gridded EchoTop_18 value (Fig. 6). Bear in mind the limitation that if the storm is fast moving or tilted, the highest Echo Top and VIL may not be co-located in the same grid square. To combat this problem, several new products are prototyped (see later sections).

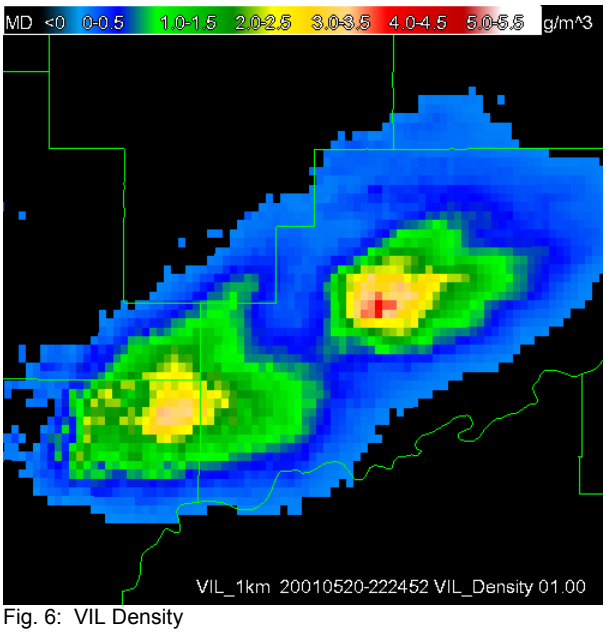

Fig. 6: VIL Density

3.4 Severe Hail Index (SHI)

This version of SHI is computed using the same cell-based equations in Witt et al (1998) except that it is vertically-integrated on a multiple-radar 3D grid (Fig. 7a). Thermodynamic data (0°C and -20°C) are integrated from the RUC20 grids. Gridded Probability of Severe Hail (POSH; Fig 7b) and Maximum Expected Hail Size (MEHS; Fig. 7c) are derived from SHI using the equations in Witt et al (1998). SHI divided by the 18 dBZ Echo Top, an analog to VIL Density, is called SHI Flux (g s^{-1}), and is shown in Fig. 7d.

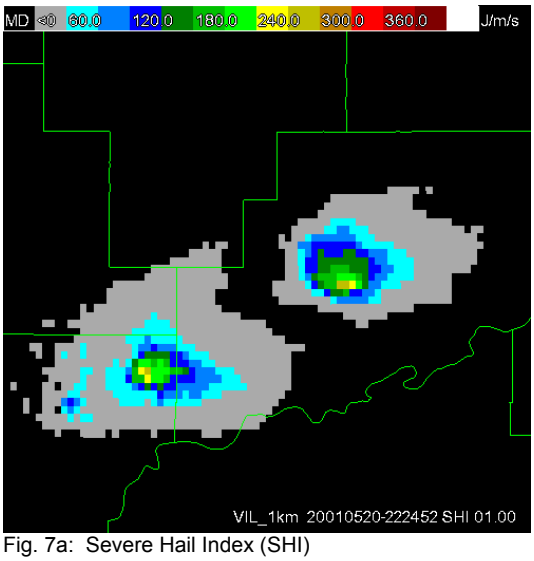

Fig. 7a: Severe Hail Index (SHI)

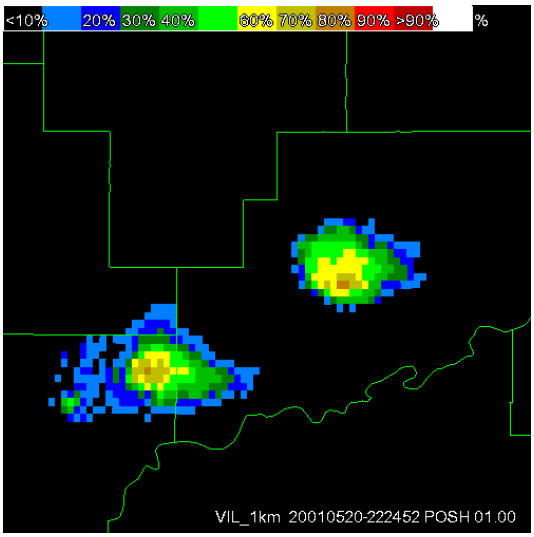

Fig. 7b: Probability of Severe Hail (POSH)

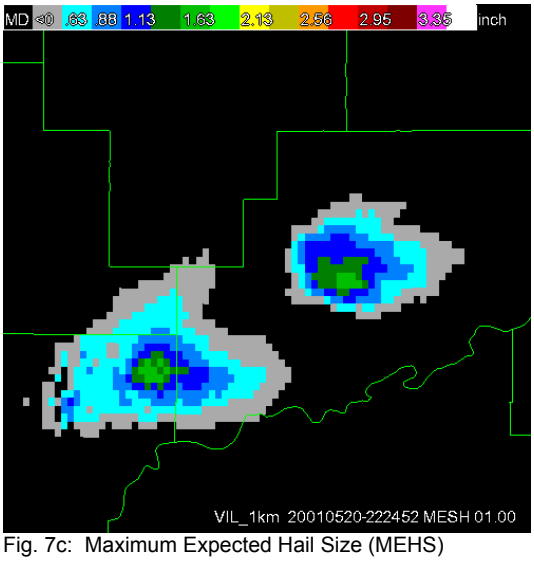

Fig. 7c: Maximum Expected Hail Size (MEHS)

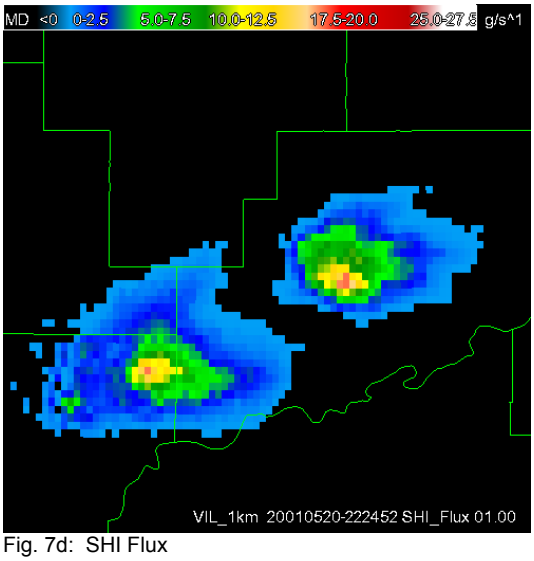

Fig. 7d: SHI Flux

Having the hail diagnosis data in grid form allows for data can be accumulated over time to produce "hail swath" products. For example, Fig. 7e shows the plotted maximum MEHS over a 120 min period ending 232952 UTC 20 May 2001. Accumulating the SHI value over time provides a proxy for Hail Damage Potential (HDP; Fig. 7f; same time period as in Fig. 7e). Higher HDP values correspond to a combination of hail size and duration of hail fall. This geospatial hail information provides much more detail on the locations of the largest hail within a storm versus just single values per storm cell. These products are very useful for determining locations of the largest hail fall for NWS warning verification as well as for emergency and insurance response. [As of this study, a gridded version of the EHDA (Marzban and Witt 2002) has not been developed.]

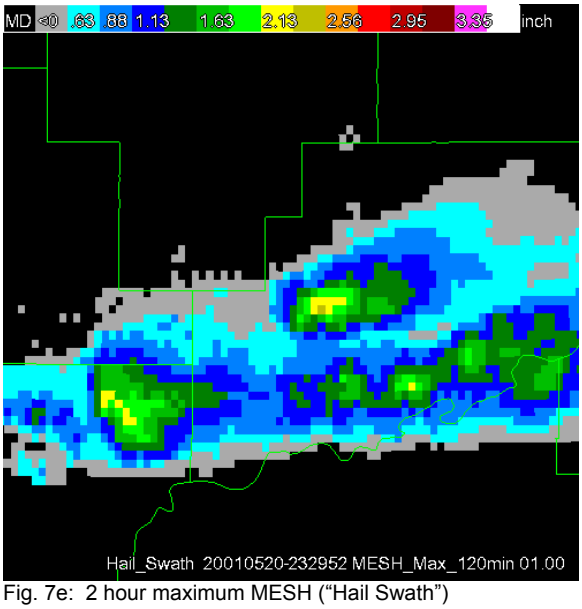

Fig. 7e: 2 hour maximum MESH ("Hail Swath")

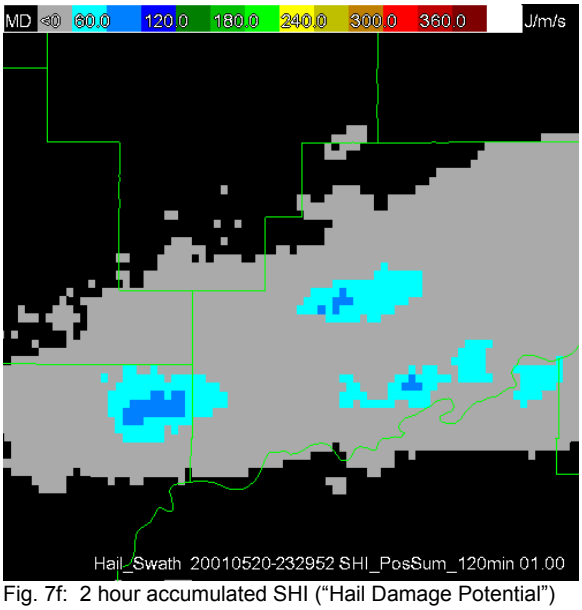

Fig. 7f: 2 hour accumulated SHI ("Hail Damage Potential")

3.5 Grids of "other popular parameters synthesized from manual base data interpretation"

New multiple-radar and multiple-sensor grids have been developed. These include Maximum Reflectivity in the vertical column, also known as "Composite Reflectivity" (Fig. 8a), Height of the Maximum Reflectivity (Fig. 8b; note the echo overhangs), Reflectivities at the 0°C and -20°C levels (Fig. 9a and 9b), and Height of the 50 dBZ level above both the 0°C and -20°C levels (Figs. 9c and 9d).

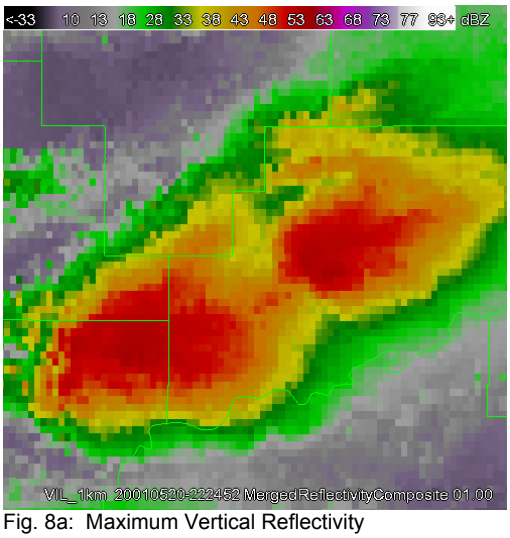

Fig. 8a: Maximum Vertical Reflectivity

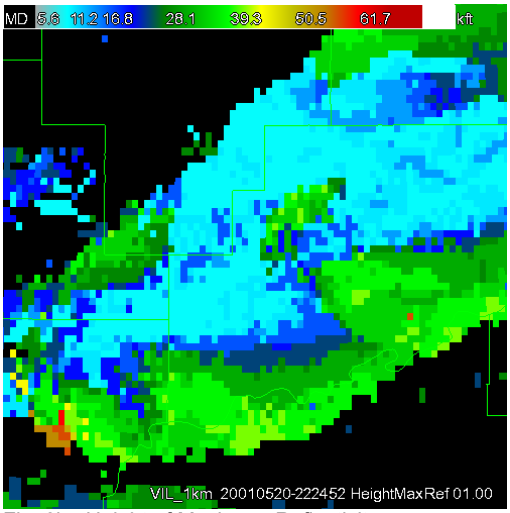

Fig. 8b: Height of Maximum Reflectivity

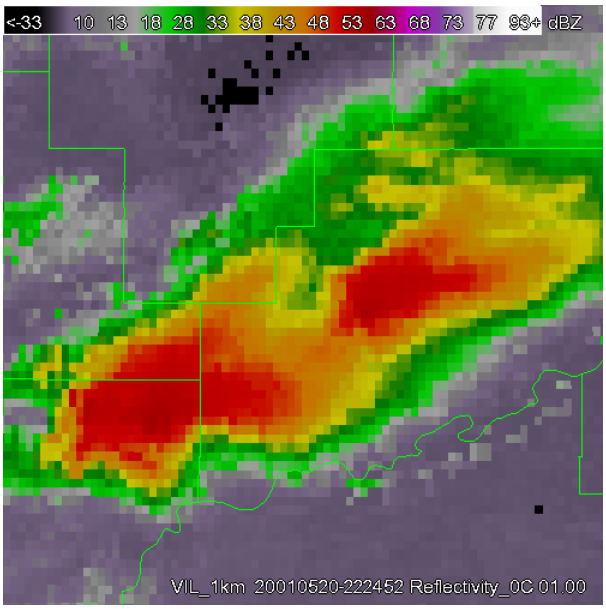

Fig. 9a: Reflectivity at 0°C

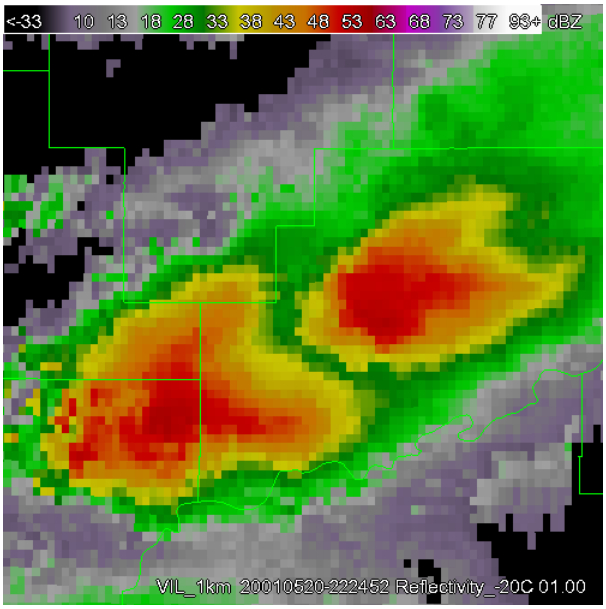

Fig. 9b: Reflectivity at -20°C

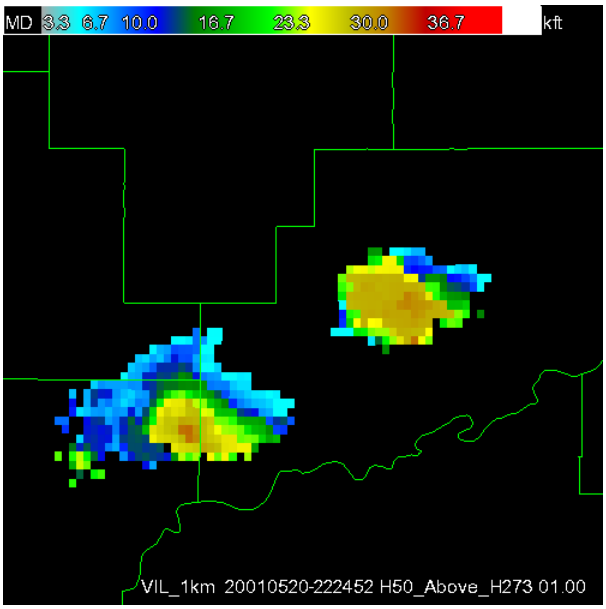

Fig. 9c: Height of 50 dBZ level above 0°C level

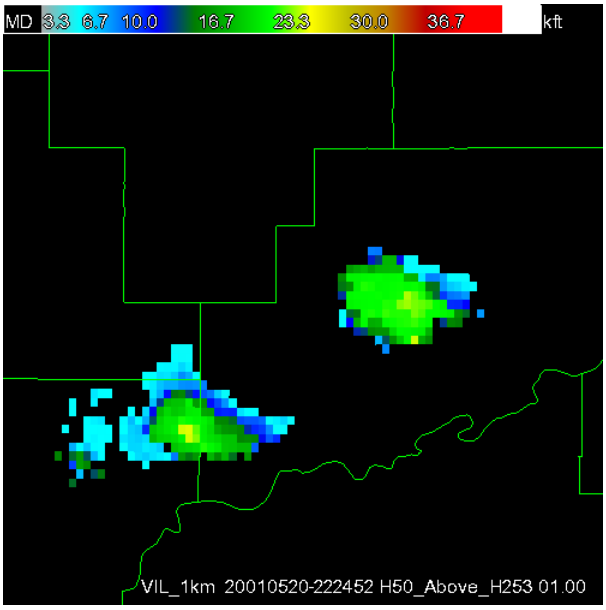

Fig 9d: Height of 50 dBZ level above -20°C level

3.6 Reconciling storms whose cores are tilted in the vertical

Several methods have been prototyped to deal with storm tilt caused by fast-moving or highly-sheared storms.

3.6.1 Dilation of VIL and EchoTop_18 fields

Morphological dilation is performed on both the VIL and the EchoTops_18 fields prior to the determination of VIL Density. To dilate the gridded data, a 5 × 5 pixel kernel is passed over every data point, and the second largest value of all the points (25 points total) in the kernel replaces the value at the center of the kernel on the original grid. One exception is that if the center grid point is the maximum of all the values in the kernel, it is not replaced with the second largest. If the center grid point contains missing data, the dilated value is set to missing. Also, the 5 × 5 kernel must comprise at least 33% non-missing values in order to compute the dilated value. If not, then the dilated value is set to missing. This procedure as the effect of increasing the reflectivity values in the neighborhood around local maxima but without expanding the original size of the reflectivity echoes. By dilating both the VIL and EchoTops_18 field, you increase the likelihood of having the maximum VIL and Echo Top aligned vertically. The overall result is that values of the VIL Density from dilation may increase (if the dilated VIL values increase) or decrease (if the dilated Echo Tops values increase). The dilated VIL field is shown in Fig 10a, the dilated EchoTop_18 field in Fig. 10b, the original VIL Density Field in Fig 11a (same as Fig. 6), and the VIL Density field from the dilated VIL and EchoTops_18 fields in Fig. 11b.

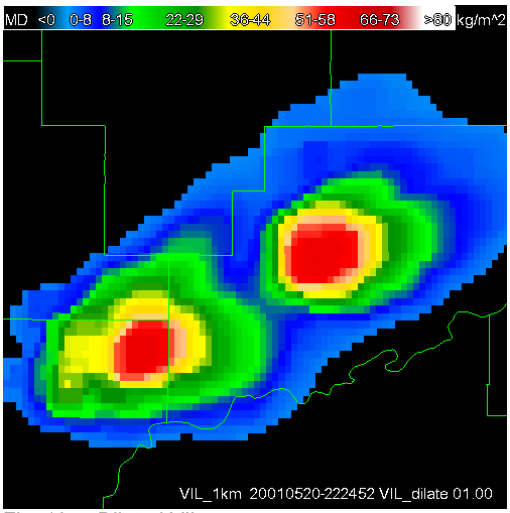

Fig. 10a: Dilated VIL

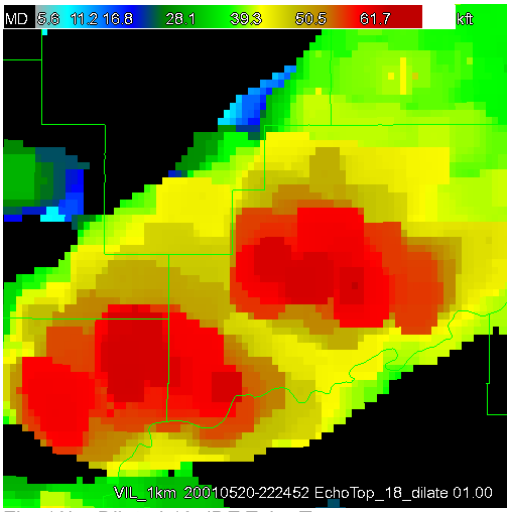

Fig. 10b: Dilated 18 dBZ Echo Tops

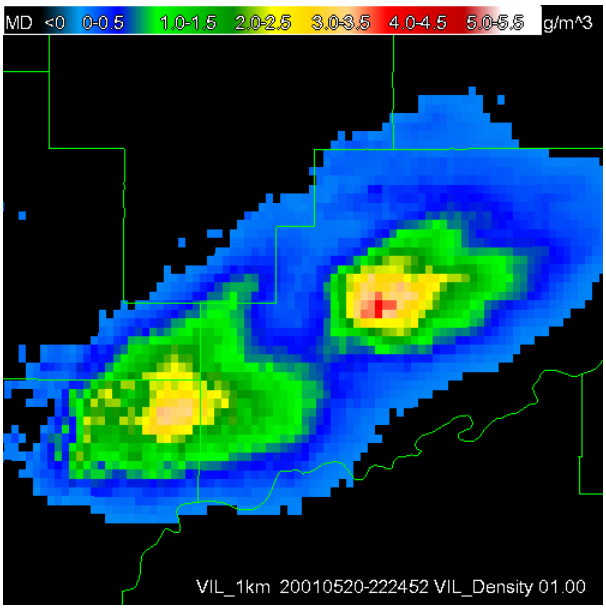

Fig. 11a: VIL Density (same as Fig. 6)

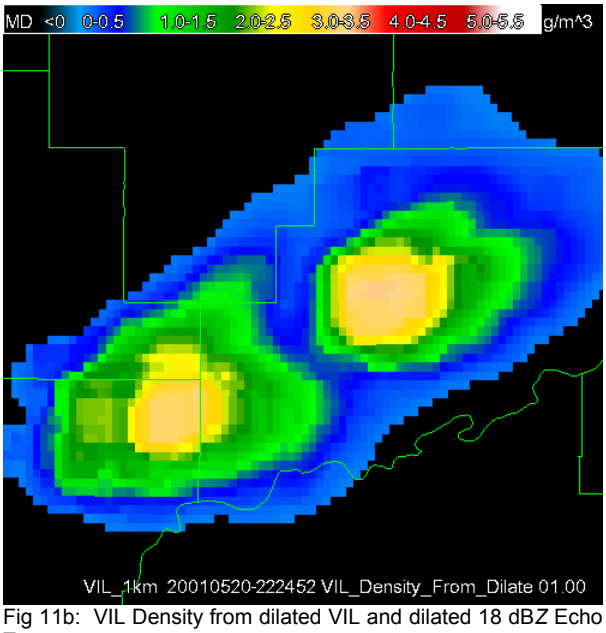

Fig 11b: VIL Density from dilated VIL and dilated 18 dBZ Echo Tops

3.6.2 Dilation of the VIL Density Field

Morphological dilation is performed on the original VIL Density field that was computed from the non-dilated VIL and non-dilated EchoTops_18 fields for comparison purposes (Fig. 12). It appears that this field is not as clean as the VIL Density from dilation field (note the 5 km × 5 km "blocky areas"), and really does not take into account any storm tilt, therefore it is not recommended.

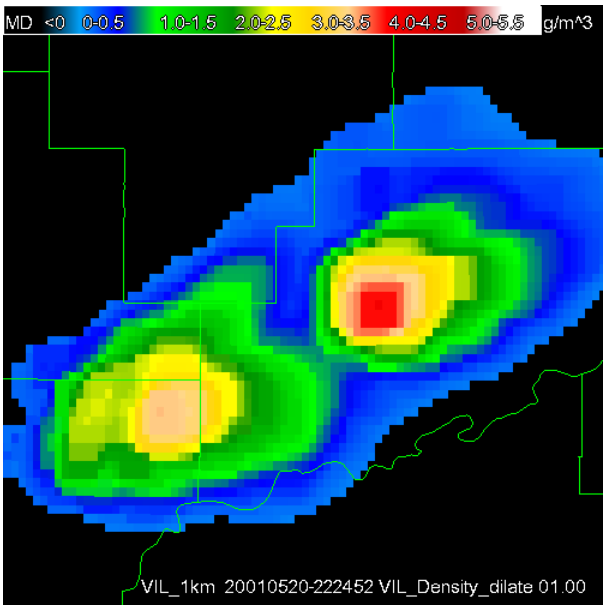

Fig. 12: Dilated VIL Density

3.6.3 Dilation of original reflectivity fields at each vertical level prior to computation of VIL, Echo Tops, VIL Density, or SHI.

This may make for a more robust VIL product that is both high-resolution, as well as allows for the "larger" grid size in the traditional 4 km × 4 km VIL product (Fig 13). It is recommended that this also be tested on the HRVIL product. VIL computed from dilated reflectivity fields is shown in Fig. 14b (original VIL is Fig 14a – same as Fig 5a), as well as EchoTops_18 (Fig. 14c), VIL Density (Fig. 14d), SHI (Fig. 14e), and MEHS (Fig. 14f), all computed using dilated reflectivity fields.

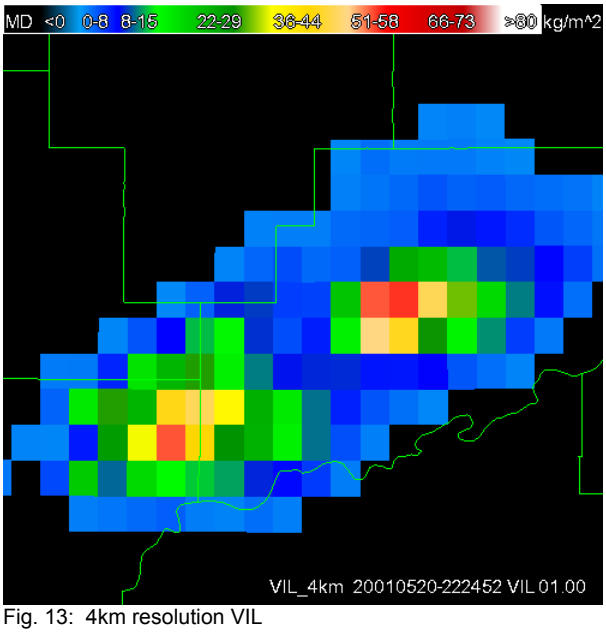

Fig. 13: 4km resolution VIL

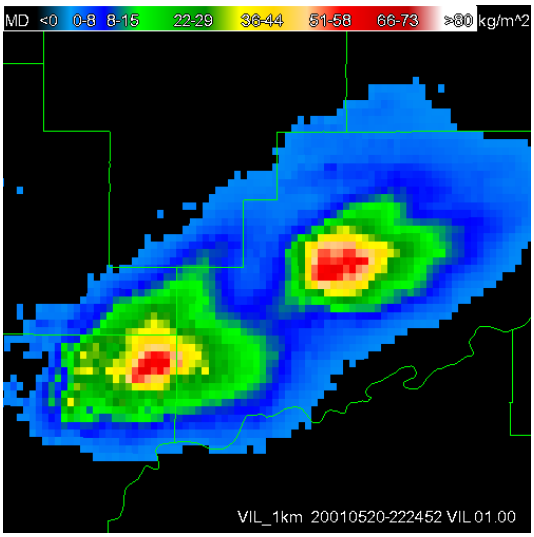

Fig. 14a: 1 km resolution VIL (same as Fig. 5)

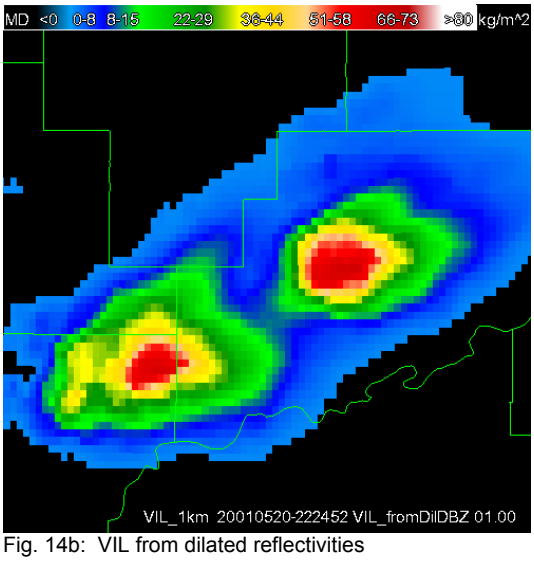

Fig. 14b: VIL from dilated reflectivities

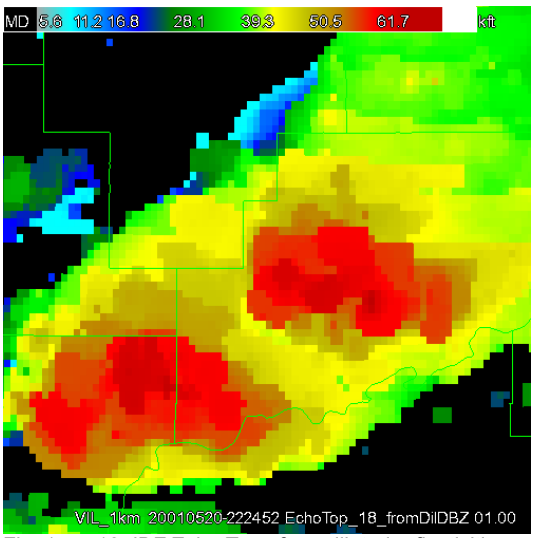

Fig. 14c: 18 dBZ Echo Tops from dilated reflectivities

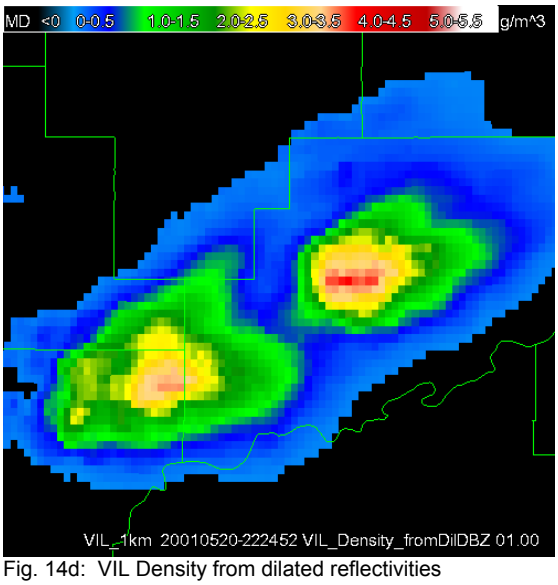

Fig. 14d: VIL Density from dilated reflectivities

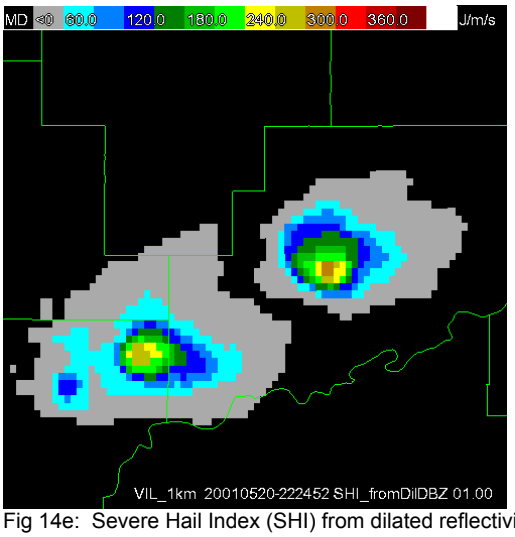

Fig 14e: Severe Hail Index (SHI) from dilated reflectivities

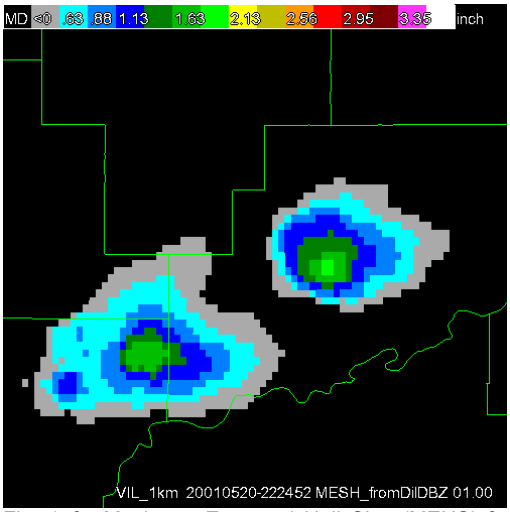

Fig. 14f: Maximum Expected Hail Size (MEHS) from dilated reflectivities

3.6.4 TILTED VERTICAL INTEGRATION

This is a relatively new concept that can have some rewarding benefits for operational meteorologists trying to sort out all the various available storm parameters (e.g., gridded versus cell-based). While the cell-based VIL and SHI products are based on integration of maximum axis of the core (takes into account the core tilt), there are still limitations with the centroid-based heuristics of the algorithms that might make for incomplete vertical cores and tracks, as well as output only available for one cell as a whole. While the present gridded VIL and SHI products provide geospatial information (location of maximum within storms) and allow for time accumulation of products (hail swaths), the integrations aren't explicitly taking into account storm core tilt in the vertical. Integration along a tilted column is the most robust method of the several outlined here, as the integration is performed along the storm core tilts explicitly rather than implicitly through image dilation. Dilation also may have the unwanted effect of combining multiple smaller cores in close proximity (multi-cell storms) since the dilation is done in all surrounding directions and not just in the direction of the storm core tilt.

Prototyped is a new method for performing the integration of reflectivity along a pre-determined 3D slope (both north-south and east-west slopes are considered) in the vertical. Presently, for the prototype, the storm tilt was determined manually from the supercells under analysis and hardwired into the code; the values chosen were for a storm core tilt of about 22° from the vertical, and tilted toward a 135° azimuth (toward the southeast). The original VIL from Fig. 5 is repeated in Fig. 15a, and in Fig. 15b is the VIL from the tilted integration. Note that the VIL fields appear cleaner and more robust and are higher overall for the storms. Also shown is the VIL Density (Fig. 15c) as computed using the "tilted" VIL and a "tilted" EchoTop_18 product. For all the "tilted" products, the integrated values are projected on the grid square at the lowest elevation of the tilted column. In the case of these supercells, the highest VILs are co-located with the highest cores on the surface, as the trajectory of the precipitation particles is eventually toward that direction in an Eulerian reference frame. SHI, POSH, and MEHS are also derived from tilted integration (figures not shown).

Several methods for automatically determining storm tilt are being considered. These include determination from a new gridded SCIT algorithm (much more stable than the centroid-based single-radar SCIT) as well as determination using environmental data (combination of mean shear and instability).

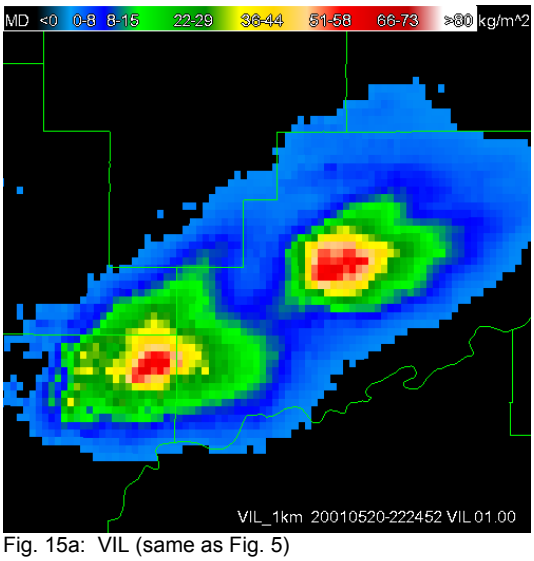

Fig. 15a: VIL (same as Fig. 5)

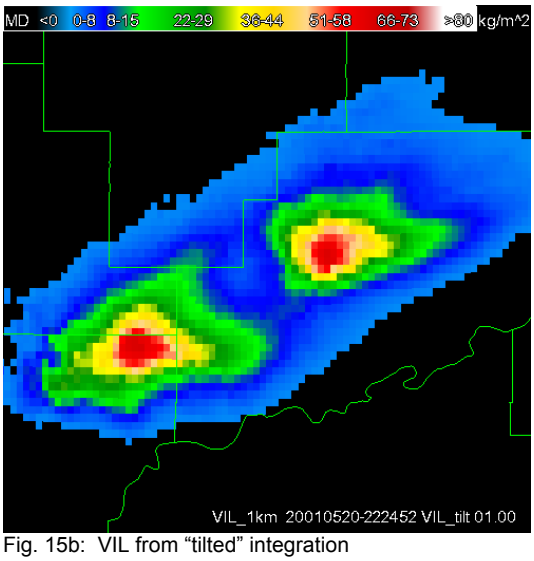

Fig. 15b: VIL from "tilted" integration

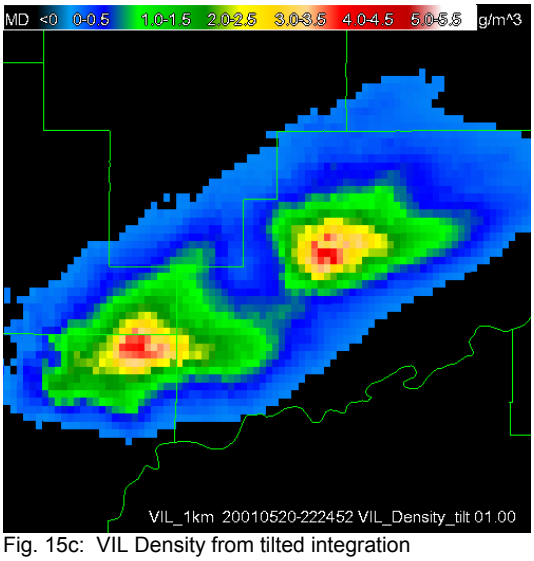

Fig. 15c: VIL Density from tilted integration

4. FUTURE CONSIDERATIONS

WDSSII was used to rapidly prototype these concepts and develop the applications. Still required is a verification study to compare all these methods (old and new) with actual hail truth data. There are possibilities for collaboration with NSSL meteorologists and students as well as WFO meteorologists to evaluate these new products using a number of storm cases. Desired are storm cases that are under-sampled by single radars but better sampled by multiple radars, as well as cases in which there are strong spatial and temporal gradients in the environmental thermodynamic characteristics.

Work should be performed to determine the relationship between shear and instability environmental parameters and observed storm tilt. This can be greatly facilitated using WDSSII and the cases developed for the hail diagnosis.

An alternative to VIL is proposed by Boudevillain and Andreau (2003) which accounts for the differences in reflectivity factor above and below the melting layers. This method should also be explored and an application developed that integrates NSE data to determine melting layers.

Simultaneously, these new hail diagnosis products can be tested in a real-time operational setting at a WFO, so that meteorologists can provide feedback on the operational utility of the new applications prior to integration into NWS operational systems. The NSSL WDSSII was used as a proof-of-concept testbed for these and other new multiple-sensor severe weather warning applications both at the Norman, Oklahoma, and Wichita, Kansas WFOs during the 2004 convective season.

5. ACKNOWLEDGMENTS

Thanks go to the NSSL WDSS-II development team of Kurt Hondl, V. Lakshmanan, Robert Toomey, Lulin Song, Charles Kerr, and Jeff Brogden. Don Burgess and Arthur Witt (NSSL) and Jim LaDue (NWS/WDTB) provided helpful comments for this work. Steve Smith (NWS/MDL) provided comments on the manuscript. This work has been primarily funded under NOAA-OU Cooperative Agreement #NA17RJ1227.

6. REFERENCES

Amburn, S. A., and P. L. Wolf, 1997: VIL density as a hail indicator. Wea. Forecasting, 12, 473-478.

Blaes, J. L., C. S. Cerniglia Jr., and M. A. Caropolo, 1998: VIL Density as an indicator of hail across Eastern New York and Western New England. *NWS Eastern Region Technical Attachment ER/SSD 98-8,* Upton, NY.

Billet, J., M. DeLisi, and B.G. Smith, 1997: Use of regression techniques to predict hail size and the probability of large hail. *Wea. Forecasting*, **12**, 154-164.

Boudevillain, B., and H. Andreau, 2003: Assessment of Vertically Integrated Liquid (VIL) Water Content Radar Measurement. *J. Atmos. Oceanic Tech.*, **20**, 807-819.

Edwards, R., and R. L. Thompson, 1998: Nationwide Comparisons of Hail Size with WSR-88D Vertically Integrated Liquid Water and Derived Thermodynamic Sounding Data. *Wea. Forecasting*, **13**, 277-285.

Greene, D. R., and R. A. Clark, 1972: Vertically integrated liquid water – A new analysis tool. Mon. Wea. Rev., 100, 548-552.

Hart, P. A., and K. D. Frantz, 1998: A comparison of VIL density and wet-bulb zero height associated with large hail over North and Central Georgia. *NWS Southern Region Technical Attachment SR/SSD 98-30*. Fort Worth, TX.

Hondl, K., 2002: Current and planned activities for the Warning Decision Support System – Integrated Information (WDSS-II). *Preprints, 21st Conference on Severe Local Storms*, San Antonio, Texas, Amer. Meteor. Soc., 146-148.

Johnson, J. T., P. L. MacKeen, A. Witt, E. D. Mitchell, G. J. Stumpf, M. D. Eilts, and K. W. Thomas, 1998: The Storm Cell Identification and Tracking (SCIT) algorithm: An enhanced WSR-88D algorithm. *Wea. Forecasting*, **13**, 263-276.

Lakshmanan, V., 2002: WDSSII: an extensible, multi-source meteorological algorithm development interface. *Preprints, 21st Conf. on Severe Local Storms*, San Antonio, Texas, Amer. Meteor. Soc., 134-137

Lenning, E., H. E. Fuelberg, and A. I. Watson, 1998: An evaluation of WSR-88D severe hail algorithms along the northeastern Gulf Coast. *Wea. Forecasting*, **13**, 1029-1044.

Marzban, C., and A. Witt, 2002: A Bayesian Neural Network for Severe-Hail Size Prediction. *Wea. Forecasting*: **16**, pp. 600–610.

Roeseler, C. A., and L. Wood, 1997: VIL density and associated hail size along the Northwest Gulf Coast. *Preprints, 28th Conf. On Radar Meteorology*, Austin, Texas, Amer. Meteor. Soc., 434-435.

Troutman, T. W. and M. Rose, 1997: An examination of VIL and echo top associated with large hail in Middle Tennessee. *NWS Southern Region*

Technical Attachment SR/SSD 97-15. Fort Worth, TX.

Turner, R. J., and D. M. Gonsowski, 1997: A review of VIL density performance at NWSO Goodland, Kansas. *Preprints, 28th Conf. On Radar Meteorology*, Austin, Texas, Amer. Meteor. Soc., 370-371.

Witt, A., M. D. Eilts, G. J. Stumpf, J. T. Johnson, E. D. Mitchell, and K. W. Thomas, 1998: An enhanced hail detection algorithm for the WSR-88D. *Wea. Forecasting*, **13**, 286-303.

Witt, A., 2000: The WSR-88D Hail Detection Algorithm: A performance update. *Preprints, 20th Conf. on Severe Local Storms*, Orlando, Florida, Amer. Meteor. Soc., 378-381.